euspen's 22nd International Conference & Exhibition, Geneva, CH, May/June 2022
www.euspen.eu

High torsion stiffness leafspring flexure element using distributed warping constraints

Marijn Nijenhuis, Mark Naves, Dannis Brouwer

Precision Engineering, Faculty of Engineering Technology, University of Twente, Enschede, The Netherlands

m.nijenhuis@utwente.nl

Abstract
Leafsprings are commonly used in flexure mechanisms to enable repeatable motion and provide support stiffness. In various applications, the torsional stiffness needs to be increased. This paper presents the concept of using warping constraints distributed along the leafspring to increase the torsional stiffness relative to the stiffness in other directions. A beam-based model of nonuniform torsion is used to estimate the relationship between the geometrical design parameters and the expected increase in torsional stiffness. The model predicts that an order of magnitude increase in stiffness is feasible. Compared to other solutions, the distributed warping constraints have a less obtrusive shape that offer more design freedom.

Flexure mechanism, leaf spring, warping, torsion stiffness, twisting, constraints

1. Introduction

Leafsprings are common components of flexure mechanisms [1-5]. Their slender shape enables repeatable motion in the three directions of low stiffness, while constraining motion in the three directions of high stiffness. As the torsional stiffness is relatively low, twisting motion is generally considered one of the three unconstrained degrees of freedom (DOFs). In some applications, it may be desirable to increase the torsional stiffness of the leafspring relative to the stiffness in the two other DOFs.

In this paper, we present the use of distributed warping constraints to significantly increase the torsional stiffness relative to the stiffness in the other directions, essentially yielding a torsionally stiffened leafspring with only two DOFs remaining.

These warping constraints may eliminate the need for additional flexures that would otherwise serve as torsional constraints. Other applications are flexure mechanisms with a large range of motion, in which the support stiffness tends to deteriorate with deflection due to unwanted torsional compliance.

Existing solutions for increasing the torsional stiffness include reinforced midsections [5], the infinity flexure [6-7] and a cell-based metamaterial [8]. Compared to these solutions, the distributed warping constraints of the present work have a less obstructive shape, offering more design freedom and application-specific tailoring.

This paper establishes the design concept and provides a theoretical model for the mode of action and the design parameters that are involved.

2. Warping

A leafspring can be considered as a slender structure with rectangular cross-sections. When it is subjected to a torsional moment, the cross-sections rotate and warp [9-10]. The warping of the cross-section is of interest, because it affects the torsional stiffness of the leafspring and it can be influenced by design choices.

If all cross-sections are free to warp, the torsion angle changes linearly over the length of the beam. However, if a cross-section is constrained from warping, additional normal and shear stresses develop in the vicinity of the constraint. These stresses require additional torque for the same torsion angle and essentially increase the torsional stiffness.

Warping can be constrained by a section with a large warping stiffness, such as the clamps or fillets commonly present at the ends of a leafspring. Since the additional stresses in the leafspring vanish at a distance from the warping constraint, the effect on the torsional stiffness is nontrivial and dependent on geometrical parameters.

3. Beam-based stiffness model

When the additional stresses due to warping constraints are significant, the torsion angle no longer changes linearly over the length of the beam and the St. Venant uniform torsion model loses validity. Instead, the torsion angle $\phi_x(s)$ can be modeled by the ordinary differential equation [9-11]

$$GJ\frac{d^2\phi_x}{ds^2} - EI_w\frac{d^4\phi_x}{ds^4} = 0 \quad (1)$$

where E is Young's modulus, G the shear modulus and s the coordinate along the beam's neutral line ranging from 0 to L. The St. Venant torsion constant for a wide rectangular beam with width w and thickness t can be approximated by

$$J \approx \frac{1}{3}wt^3 \quad (2)$$

and the warping constant by

$$I_w \approx \frac{1}{144}w^3t^3 \quad (3)$$

The torsional moment at a position s is given by

$$M_x(s) = GJ\frac{d\phi_x}{ds} - EI_w\frac{d^3\phi_x}{ds^3} \quad (4)$$

The quantity

$$B(s) = EI_w\frac{d^2\phi_x}{ds^2} \quad (5)$$

is referred to as the bimoment and represents the stress resultant associated with the additional stresses due to warping constraints. If warping is free, then $B = 0$. If warping is perfectly constrained, i.e. with infinite warping stiffness, then $\phi_x' = 0$, where a prime denotes differentiation with respect to s.

To obtain the stiffness matrix, the ODE can be solved for the torsion angle by supplying the four boundary conditions

$$\phi_x(0) = \Phi_0 \qquad \phi_x(L) = \Phi_L$$
$$\phi_x'(0) = W_0 \qquad \phi_x'(L) = W_L$$

The stiffness matrix can be found by substituting the solution for $\phi_x(s)$ in equations 4 and 5, and evaluating the torsional moment and bimoment at both ends $s = 0$ and $s = L$. This yields

$$\begin{bmatrix} M_0 \\ M_L \\ B_0 \\ B_L \end{bmatrix} = \boldsymbol{K} \begin{bmatrix} \Phi_0 \\ \Phi_L \\ W_0 \\ W_L \end{bmatrix} \tag{6}$$

The full expression of stiffness matrix $\boldsymbol{K}$ is given in the appendix. Each matrix component depends on G, J, L and λ. Here, the dimensionless parameter λ has been introduced. It is given by

$$\lambda = L\sqrt{\frac{GJ}{EI_w}} \approx \frac{L}{w}\sqrt{\frac{24}{1+\nu}} \tag{7}$$

and relates the warping stiffness EI_w to the uniform torsion stiffness GJ. It can be interpreted as a spatial decay rate for the warping stresses.

For the present discussion, we isolate component 2,2 ($dM_L/d\Phi_L$) from $\boldsymbol{K}$ and consider it to be the torsional stiffness in the presence of perfect warping constraints at both ends (i.e. $W_0 = W_L = 0$). It is given by

$$k_x = \frac{GJ}{L}\left(\frac{\lambda}{\lambda - 2\tanh\left(\frac{\lambda}{2}\right)}\right) \tag{8}$$

Since the torsional stiffness in the case of free warping is GJ/L, we can see that the warping constraints lead to a stiffening factor of

$$\gamma = \frac{\lambda}{\lambda - 2\tanh\left(\frac{\lambda}{2}\right)} \tag{9}$$

as shown in figure 1 for L/w ratios from $1/4$ to 15 and $\nu = 0.3$. This range corresponds with λ from 1 to 64. It can be seen that the stiffness remains unaffected for slender beams with a large L/w ratio (i.e. a large decay rate λ), but strongly increases for shorter beams.

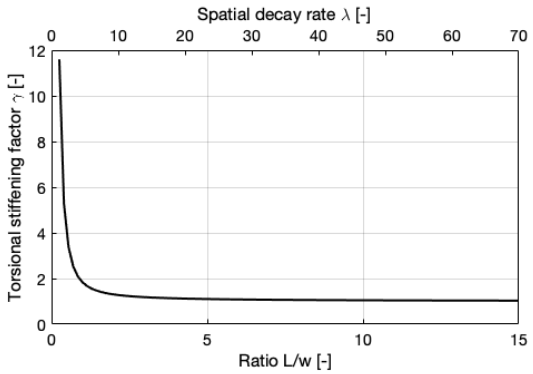

Figure 1. Increase in torsional stiffness due to constrained warping, based on a beam model for nonuniform torsion in leafsprings.

4. Distributed warping constraints

This paper introduces the idea of using a number of warping constraints distributed along the leafspring's length dimension, in order to increase the total torsional stiffness. Each warping constraint represents a local increase in warping stiffness that hinders torsional deformation. This reinforced leafspring can be regarded as a series of very short clamped-clamped leafspring segments with warping constrained at both ends. Each segment has a small spatial decay rate λ (i.e. a small length-to-width ratio), such that the warping stresses cannot significantly diminish over the length of the segment.

Figure 2 shows a 3D-printed prototype of a 150 x 50 x 1 mm leafspring with 14 local warping constraints, effected by 14 segments of 20 x 2 mm distributed equally along the length.

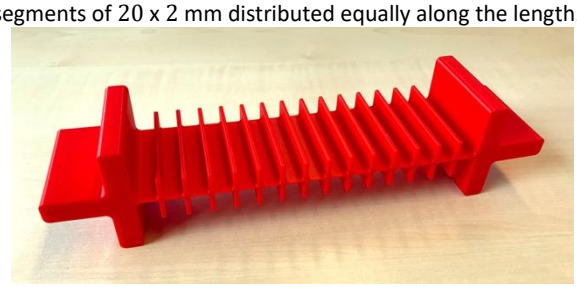

Figure 2. Photograph of a leafspring with distributed warping constraints.

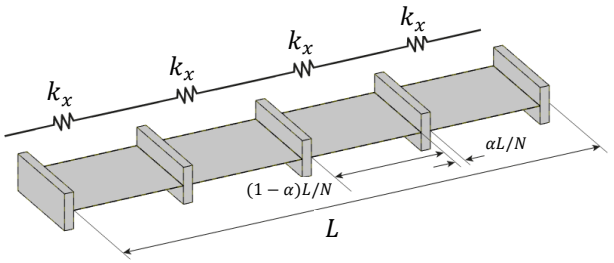

Figure 3. Schematic of the leafspring with distributed warping constraints.

4.1. Perfect-constraint model

The theoretical stiffness increase, an upper bound based on the perfect-constraint model of the previous section, can be obtained by considering the reinforced leafspring as a series connection of N individual torsion compliances $1/k_x$, see figure 3. The length of each segment is L/N. Each segment is comprised of the warping constraint with length $\alpha L/N$ and a flexible part with length $(1-\alpha)L/N$. With this definition, α represents the fraction of the total leafspring length L that is used by the warping constraints.

The total stiffness of the reinforced leafspring is given by the reciprocal sum

$$k_{x,\text{reinf}} = \left(\frac{1}{k_{x,1}} + \cdots + \frac{1}{k_{x,N}}\right)^{-1} \tag{10}$$

which, for identical segments, reduces to

$$k_{x,\text{reinf}} = \frac{GJ}{L(1-\alpha)}\left(\frac{\lambda_e}{\lambda_e - 2\tanh\left(\frac{\lambda_e}{2}\right)}\right) \tag{11}$$

This expression takes the same form as the one for the regular leafspring (equation 8). Parameter L still represents the total length of the full leafspring, but now the stiffening factor (figure 1) for the *entire reinforced leafspring* is dependent on λ_e, which is the decay rate of *a single segment*. It is given by

$$\lambda_e = \frac{L(1-\alpha)}{Nw}\sqrt{\frac{24}{1+\nu}} \tag{12}$$

Equations 11 and 12 show how the design parameters affect the stiffness increase that can be obtained with the reinforced leafspring. Comparing with equation 7, the ratio L/w plays the same role as for the regular leafspring, but we also see that increasing the number of constraints N drastically reduces the spatial decay rate and hence, as per figure 1, increases the torsional stiffness.

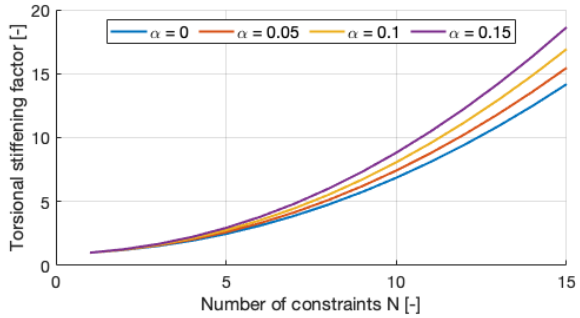

Figure 4. Torsional stiffening factor due to warping constraints, equally distributed over the leafspring.

Figure 4 shows the stiffening factor, expressed as $k_{x,\mathrm{reinf}}$ normalised with GJ/L (the stiffness in the free-warping case), for various numbers of constraints N.

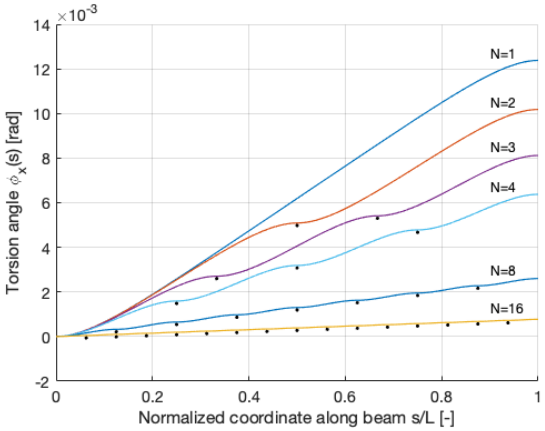

Figure 5. Profile of torsion angle $\phi_x(s)$ as a function of the length coordinate for various numbers of warping constraints N. The black dots indicate the location of the warping constraint, where locally $\phi_x' = 0$.

Figure 5 shows the torsion angle $\phi_x(s)$ as a function of the length coordinate s, based on the solution of equation 1 (see appendix). The dimensions and material parameters can be found in the appendix. Graphs for various numbers of constraints have been plotted; in all cases the same torsional moment has been applied. The warping constraint length α has been set to 0. In the free-warping case, the torsion angle varies linearly with s and achieves the largest value of all cases at the end at $s = L$. When perfect warping constraints are present, the torsion angle has zero slope locally, retarding the progression of twist, leading to smaller torsion angles at the end and to a larger stiffness.

4.2. Finite-length perfect-constraint model

Parameter α represents the length of the warping constraint segments relative to the flexible length. An ideal warping constraint would provide infinite stiffness and have zero length ($\alpha = 0$), but in reality both will be finite. When $\alpha > 0$, the effective flexible length decreases and the torsional stiffness increases (also see figure 4). While that is a desirable property, it will also lead to a larger stiffness in the two intended DOFs of the leafspring. Bending stiffness EI/L becomes $EI/(L(1-\alpha))$, which may either be acceptable or should be compensated for by a smaller thickness

$$t = \frac{2\sigma_{\max} L(1-\alpha)}{\phi_{z,\max} E} \qquad (13)$$

to ensure the same bending stress levels $\sigma_{\max}$ given a certain prescribed bending rotation angle $\phi_{z,\max}$. Similar considerations can be had for the compliant translational direction.

5. Discussion

Realistic warping constraints will have a finite length and a finite warping stiffness. As the beam-based model of section 4 assumed an infinite warping stiffness, it serves as an upper bound for the achievable stiffness increase. Some error is incurred here, since the individual segments have very small length-to-width ratios, which are pushing the limits of validity of beam theory. It is conceivable that plate-like effects, such as the nonlinear Wagner torque for larger torsion angles and constrained anticlastic bending [12-14], will play a role as well.

Stress considerations will limit the number and the length of the warping constraints that can be implemented, representing another bound on the maximally achievable stiffness increase.

The optimal shape of the warping constraints themselves has not been discussed in this paper. It will be an application-specific trade-off, since adding too much mass may hinder dynamic performance, using up too much volume may cause self-collision depending on the intended range of motion in the DOFs, and intricate shapes may be hard to manufacture, even with additive manufacturing.

Depending on the load case of the leafspring, equally spaced warping constraints may not be ideal. For instance, if the applied load is not a pure torsional moment, but instead a lateral force that causes a varying internal torsional moment when the leafspring is bent, warping constraints could be concentrated around where the torsional moment is largest. This could mitigate some of the support stiffness decrease observed in large range of motion flexures, which can be due to undesired torsional compliance [13,15].

Experiments to validate this model and design considerations for the shape of the warping constraints are topics for future work.

6. Conclusion

This paper has presented the concept of using warping constraints distributed over a leafspring's length to increase the torsional stiffness relative to the stiffness in other directions. A theoretical foundation has been established by means of a beam-based stiffness model. The model predicts that a stiffening factor of an order of magnitude is feasible. Reinforcing leafsprings this way can be useful since the warping constraints offer a lot of design freedom that can be leveraged for the specifics of an application. It has practical relevance since there are numerous flexure mechanism cases where torsional compliance is unwanted.

References

[1] Eastman F S 1935 Flexure pivots to replace knife edges and ball bearings *Engineering Experiment Station Bulletin* **86**

[2] Jones R V 1956 A parallel-spring cross-movement for an optical bench *J. Scientific Instruments* **33** 279–280

[3] Slocum A H 1992 Precision Machine Design (Prentice Hall)

[4] Smith S T 2000 Flexures: Elements of Elastic Mechanisms (CRC Press)

[5] Soemers H 2011 Design Principles for precision mechanisms (T-pointpress)

[6] Wiersma D H, Boer S E, Aarts R G K M, Brouwer D M 2013 Design and Performance Optimization of Large Stroke Spatial Flexures *J. Computational and Nonlinear Dynamics* **9**

[7] Naves M, Brouwer D M, Aarts R G K M 2017 Building Block-Based Spatial Topology Synthesis Method for Large-Stroke Flexure Hinges *J. Mechanisms and Robotics* **9** 041006–9

[8] Andree D J, Nijenhuis M, Brouwer D M 2018 Design of a meta-material for the torsional reinforcement of a leaf spring *Proceedings of The Thirty-Third Annual Meeting of the American Society for Precision Engineering* 563-568

[9] Timoshenko S, Goodier J N 1969 Theory of Elasticity (McGraw-Hill)
[10] Trahair N S 1993 Flexural-Torsional Buckling of Structures (CRC Press)
[11] Van Eijk J 1985 On the design of plate-spring mechanisms (Delft University of Technology)
[12] Nijenhuis M, Meijaard J P, Brouwer D M 2020 A spatial closed-form nonlinear stiffness model for sheet flexures based on a mixed variational principle including third-order effects *Precision Engineering* **66** 429-444
[13] Brouwer D M, Meijaard J P, Jonker J B 2013 Large deflection stiffness analysis of parallel prismatic leaf-spring flexures *Precision Engineering* **37** 505–521
[14] Meijaard J P 2011 Refinements of Classical Beam Theory for Beams with a Large Aspect Ratio of Their Cross-Sections *IUTAM Symposium on Dynamics Modeling and Interaction Control in Virtual and Real Environments* 285–292
[15] Nijenhuis M, Meijaard J P, Mariappan D, Herder J L, Brouwer D M, Awtar S 2017 An Analytical Formulation for the Lateral Support Stiffness of a Spatial Flexure Strip *J. Mechanical Design* **139**

Appendix

Torsion angle solution

The solution of the ordinary differential equation with the specified boundary conditions is given by

$$\phi_x(s) = c_1 \frac{L^2}{\lambda^2} e^{\frac{x\lambda}{L}} + c_2 \frac{L^2}{\lambda^2} e^{-\frac{x\lambda}{L}} + c_3 + c_4 x$$

where

$$c_1 = \frac{\lambda\left(L\left(-1+e^{\lambda}-\lambda\right)W_0 + L\left(1+e^{\lambda}(-1+\lambda)\right)W_L + \left(-1+e^{\lambda}\right)\lambda(\Phi_0-\Phi_L)\right)}{(-1+e^{\lambda})L^2(2+e^{\lambda}(-2+\lambda)+\lambda)}$$

$$c_2 = -\frac{e^{\lambda}\lambda\left(L\left(1+e^{\lambda}(-1+\lambda)\right)W_0 + L\left(-1+e^{\lambda}-\lambda\right)W_L + \left(-1+e^{\lambda}\right)\lambda(\Phi_0-\Phi_L)\right)}{(-1+e^{\lambda})L^2(2+e^{\lambda}(-2+\lambda)+\lambda)}$$

$$c_3 = \frac{L\left(1+e^{2\lambda}(-1+\lambda)+\lambda\right)W_0 + L\left(-1+e^{2\lambda}-2e^{\lambda}\lambda\right)W_L + \left(-1+e^{\lambda}\right)\lambda\left(\left(1+e^{\lambda}(-1+\lambda)+\lambda\right)\Phi_0 - \left(-1+e^{\lambda}\right)\Phi_L\right)}{(-1+e^{\lambda})\lambda(2+e^{\lambda}(-2+\lambda)+\lambda)}$$

$$c_4 = -\frac{(-1+e^{\lambda})LW_0 + (-1+e^{\lambda})LW_L + (1+e^{\lambda})\lambda(\Phi_0-\Phi_L)}{L(2+e^{\lambda}(-2+\lambda)+\lambda)}$$

Stiffness matrix

Stiffness matrix $\boldsymbol{K}$ is given by

$$\begin{bmatrix}
-\frac{GJ\lambda}{L\lambda-2L\tanh[\frac{\lambda}{2}]} & \frac{GJ\lambda}{L\lambda-2L\tanh[\frac{\lambda}{2}]} & \frac{GJ}{2-\lambda\coth[\frac{\lambda}{2}]} & \frac{GJ}{2-\lambda\coth[\frac{\lambda}{2}]} \\
-\frac{GJ\lambda}{L\lambda-2L\tanh[\frac{\lambda}{2}]} & \frac{GJ\lambda}{L\lambda-2L\tanh[\frac{\lambda}{2}]} & \frac{GJ}{2-\lambda\coth[\frac{\lambda}{2}]} & \frac{GJ}{2-\lambda\coth[\frac{\lambda}{2}]} \\
\frac{GJ}{2-\lambda\coth[\frac{\lambda}{2}]} & \frac{GJ}{-2+\lambda\coth[\frac{\lambda}{2}]} & \frac{GJL\operatorname{csch}[\frac{\lambda}{2}]^2(-\lambda\cosh[\lambda]+\sinh[\lambda])}{2\lambda(-2+\lambda\coth[\frac{\lambda}{2}])} & \frac{GJL\operatorname{csch}[\frac{\lambda}{2}]^2(\lambda-\sinh[\lambda])}{2\lambda(-2+\lambda\coth[\frac{\lambda}{2}])} \\
\frac{GJ}{-2+\lambda\coth[\frac{\lambda}{2}]} & \frac{GJ}{2-\lambda\coth[\frac{\lambda}{2}]} & \frac{GJL\operatorname{csch}[\frac{\lambda}{2}]^2(-\lambda+\sinh[\lambda])}{2\lambda(-2+\lambda\coth[\frac{\lambda}{2}])} & \frac{GJL\operatorname{csch}[\frac{\lambda}{2}]^2(\lambda\cosh[\lambda]-\sinh[\lambda])}{2\lambda(-2+\lambda\coth[\frac{\lambda}{2}])}
\end{bmatrix}$$

where csch represents the hyperbolic cosecant.

Figure 5 details

Leafspring dimensions are 100 x 30 x 1 mm. Young's modulus is 210 GPa. Shear modulus is 70 GPa.
The applied torsional moment is 0.1 Nm.